Effect of spin-orbit interaction on the quenching of the acoustoelectric current in a quasi-one-dimensional channel

Godfrey Gumbs* and Yonatan Abranyos†
Department of Physics and Astronomy, Hunter College at the City University of New York, 695 Park Avenue New York, New York 10021, USA
(Received 6 July 2005; revised manuscript received 31 October 2005; published 1 February 2006)

We investigate the effect that the Rashba spin-orbit (SO) coupling has on the quenching of the acoustoelectric current in a narrow channel. For an electrostatic potential $V(\mathbf{r},t)$, the SO Hamiltonian is given by $H_{SO}=[\hbar/(2m^*c)^2]\nabla V\cdot(\boldsymbol{\sigma}\times\mathbf{p})$. Here, $\mathbf{p}$ is the particle momentum and $\boldsymbol{\sigma}$ is the vector of Pauli matrices. The confining potential $V(\mathbf{r},t)$ arises from the electrostatic potential within the channel due to a powerful surface acoustic wave (SAW) launched in a piezoelectric material, plus the two-dimensional confinement at the heterojunction as well as the potential defining the narrow channel between split metal gates. Working in the adiabatic approximation, we demonstrate that the SO interaction increases the confinement of a captured electron in a moving SAW quantum dot and may consequently improve the quenching of the quantized acoustoelectric current.

DOI: 10.1103/PhysRevB.73.085303 PACS number(s): 73.23.Hk, 72.50.+b, 73.21.La

I. INTRODUCTION

Nanofabrication technology has made it possible to confine a small number of electrons electrostatically within quantum dots using a variety of techniques.[1–3] Interest in these structures has been largely stimulated by their potential use as devices in electronics. Attention is now turning to the control of the trapped electron spin which may be used as a qubit.[4,5] More recently, a new proposal was put forward by Barnes, Shilton, and Robinson[6] for spin control and possible practical applications involving quantum information processing and quantum computers following recent experiments[7–13] in which small numbers of electrons were transported using powerful surface acoustic waves (SAWs) of frequency ~3 GHz and acoustoelectric current ~0.5 nA, even in the gate voltage domain below the pinch-off voltage for conductance. (See the article by Ono *et al.*[14] for a review and list of references.) Cunningham *et al.*[15] have been able to independently control the acoustoelectric current in two adjacent quasi-one-dimensional wires in $Al_xGa_{1-x}As$-GaAs heterostructures. The achievement of this control of charge has resulted in the proposed use of the acoustoelectric current in nanocircuits. This new field of quantum spintronics may also find applications in single photon detectors[16] and high-frequency acoustoelectric single-photon sources in which an electron is transported by a SAW into a *p*-type region of a lateral *n*-*p* junction.[17,18] The success of these proposals depends crucially on the confinement of the electrons within the moving quantum dots. The rise of the current from zero to its first quantized value is due to a decrease in the rate of the backward tunneling of the captured electrons in the moving quantum dot.[19] As a matter of fact, an aim of the original experiments was to use the quantization of the acoustoelectric current to define the unit of charge.[8–13] However, the accuracy achieved was only 50 parts per million which is not acceptable as a current standard where the current in the nanoampere range must be accurate to better than one part in 10^7. In Ref. 20, a study of the shot noise in the current of SAW-based pumps was presented. This noise arises from fluctuations in the number of electrons transported by the dots or variations in the time intervals between successive pulses.[21] The low-frequency shot noise measured in Ref. 20 was attributed to switching of impurity states which arises from the exchange of electrons between single-electron traps in the heterostructure.

In Ref. 22, results of experiments were reported on how a magnetic field applied perpendicular to the plane of the two-dimensional electron gas (2DEG) affects the quantization of an acoustoelectric current in a narrow channel. The acoustoelectric current displays oscillations at low magnetic fields and have been identified as commensurability oscillations, i.e., geometric resonances between the SAW wavelength and cyclotron diameter.[23] Experiment shows that these oscillations grow weaker as the gate voltage approaches the value corresponding to the plateau in current. One of the important consequences is that the acoustoelectric current gets flatter at this value of magnetic field. Thus the effect of magnetic field serves to reduce the backward tunneling of an electron trapped in the moving SAW quantum dot. This has motivated us to investigate how the accuracy of the acoustoelectric current can be improved by the spin-orbit (SO) mechanism which was introduced by Bychkov and Rashba[24] and which is usually referred to as the Rashba or quantum well coupling. Recent experiments suggest the possibility of spontaneous spin polarization in $GaAs/Al_xGa_{1-x}As$ heterostructures.[25,26] The SO Hamiltonian can be obtained from the Dirac equation in an external electromagnetic field, described by a vector potential $\mathbf{A}$ and a scalar potential Φ, by taking the nonrelativistic limit up to terms quadratic in v/c inclusive. The Rashba SO coupling is a unique feature of the reduced dimensionality. The potential profile for the moving quantum dots has electrostatic origin and gives rise to a finite local electric field within the quantum well. Electrons in the quantum well experience a finite electric field which varies over time.[27]

The purpose of this paper is to investigate how the Rashba SO mechanism can affect the electron confinement within

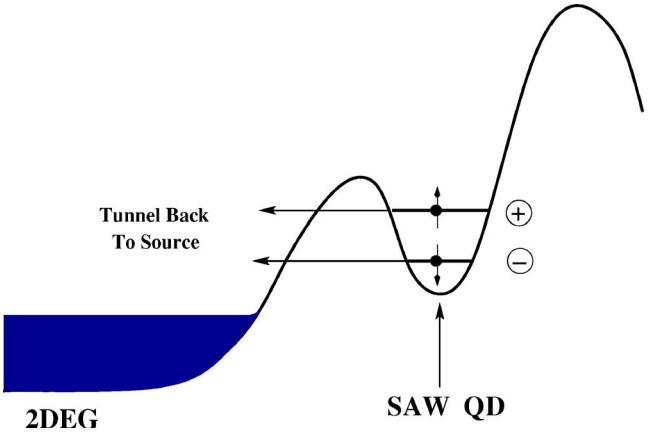

FIG. 1. (Color online) Schematic of the confining potential and probable tunneling of a captured electron from a SAW quantum dot (QD) back to the 2DEG source. The two lowest states an electron may occupy are denoted by + and − and are eigenstates of the model Hamiltonian with Rashba SO coupling.

the quantum dot formed by the electrostatic field in a piezoelectric material when a SAW is launched. When an electron is captured by the SAW, it may tunnel back to the two-dimensional electron gas through the adjacent potential barrier as shown in Fig. 1. The lower the energy level within the quantum dot, the wider is the potential barrier for the electron to tunnel through and return to the source. We demonstrate the suppression of the energy levels by the Rashba SO interaction, meaning that the electrons are more likely to be transported through the channel.

We organize the rest of this paper as follows. In Sec. II, we present our model and the formalism for calculating the energy levels of a captured electron in a moving SAW quantum dot. In Sec. III, we discuss our numerical results. Section IV is devoted to a summary.

II. SPIN-ORBIT HAMILTONIAN FOR FLYING QUANTUM DOT

A. The model

In the presence of SO interaction, the Hamiltonian for an electron with momentum $\mathbf{p}$ in the xy plane takes the following form for the geometry shown in Fig. 2:

$$H(t) = \frac{\mathbf{p}^2}{2m^*} + H_{LC} + H_B + H_{SAW}(x,t) + H_{SO}, \tag{1}$$

where m^* is the electron effective mass. In this time-dependent Hamiltonian, we consider a parabolic lateral confinement along the y axis given by

$$H_{LC} = \frac{1}{2} m^* \Omega^2 y^2, \tag{2}$$

where Ω is a constant. This potential originates from an electric field per unit charge equal to $-m^*\Omega^2\mathbf{y}$. The split gate and the SAW are described by

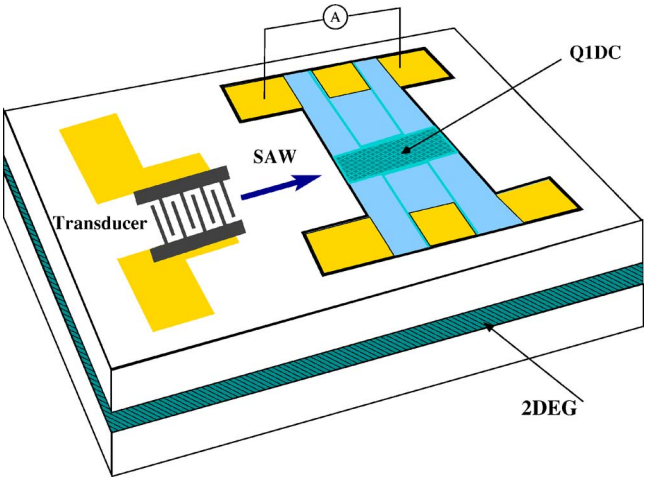

FIG. 2. (Color online) The geometry of the heterostructure device showing the two-dimensional electron gas with split metal gates on the surface of a piezoelectric heterostructure. A SAW is launched by an interdigital transducer to transport electrons through a quasi-one-dimensional channel (Q1DC).

$$H_B + H_{SAW}(x,t) = \frac{V_0}{\cosh^2(x/\ell)} + V_{SAW}\cos(kx - \omega t), \tag{3}$$

where k is the wave number and ω the frequency of the SAW of amplitude V_{SAW}. Also, ℓ is the length of the channel and V_0, the potential barrier within the channel, is assumed much larger than the Fermi energy when the quasi-one-dimensional channel is pinched off. Finally, the SO interaction term given in terms of the vector of Pauli spin matrices, i.e., $\vec{\sigma} = (\sigma_x, \sigma_y, \sigma_z)$, is

$$H_{SO} = \frac{\hbar}{(2m^* c)^2} \nabla V(\mathbf{r}) \cdot (\boldsymbol{\sigma} \times \mathbf{p}), \tag{4}$$

where $V(\mathbf{r})$ may be the electrostatic potential energy due to an electric field. In a bulk semiconductor, $V(\mathbf{r})$ arises from the periodic crystal potential. Most multicomponent III-V semiconductors lack inversion symmetry. Dresselhaus[28] has shown that this leads to a SO-induced splitting of the conduction band into two subbands and that the magnitude of this splitting is proportional to the cube of the wave number k. For a heterostructure, the crystal symmetry is broken at the interface where 2D electrons or holes are confined in a quantum well. Consequently, the host 3D crystal cannot be considered as ideal. In fact, the symmetry of the underlying crystal is lowered by the reduction of the dimensionality and gives rise to an additional term in the energy which is linear in k for the Dresselhaus splitting. The linear term is dominant for a sufficiently narrow quantum well.[29–31] Thus, the form given in Eq. (4) is not restricted to a particular model of the potential $V(\mathbf{r})$. In general, Eq. (4) consists of three terms arising from the spatial confinement. The z component gives rise to the Rashba term for an asymmetric quantum well. Furthermore, there is lateral confinement which gives additional contributions to the Hamiltonian. Taking account of the electric field within the quantum well in the direction perpendicular to the interface of the heterojunction, as an

average, the SO Hamiltonian (4) can be rewritten for the Rashba coupling as follows:

$$H_{SO}^{\alpha} = i\alpha\left(\sigma_y \frac{\partial}{\partial x} - \sigma_x \frac{\partial}{\partial y}\right), \tag{5}$$

$$H_{SO}^{\beta} = i\beta \frac{y}{\lambda_0}\sigma_z \frac{\partial}{\partial x}, \tag{6}$$

$$H_{SO}^{\gamma} = i\gamma(x,t)\sigma_z \frac{\partial}{\partial y}. \tag{7}$$

Here, $\lambda_0 = \sqrt{\hbar/m^*\Omega}$ is a characteristic length of the lateral harmonic potential. Confinement in the z direction leads to the Rashba α term and the lateral parabolic confinement results in the β term. Finally, the split-gate and SAW potentials give rise to the γ term. The coefficient γ is time dependent due to the confining potential formed by the SAW and the potential barrier in the pinched-off channel. Its spatial variation is determined by the potential in Eq. (3). We now turn to a discussion of the single-particle states of our Hamiltonian in the adiabatic approximation. Adiabatic pumping of electrons by means of a time-dependent electrostatic potential and time-varying Rashba effects have been discussed in Refs. 32 and 33, respectively. In addition, nonadiabatic pumping in a ballistic narrow constriction has been discussed in Ref. 10. The SAWs used in the experiments of Ref. 34 have a frequency of $\sim$3 GHz and a wavelength $\lambda \approx 1.0$ μm. The adiabatic approximation is valid when the change in the external parameters of the Hamiltonian is slow compared to the intrinsic time of the quantum system. In this case, the external time is characterized by frequency of the SAW which is $\sim$3 GHz. The internal time is described by $|E_n - E_m|/\hbar$ where in our case $E_n - E_m \sim 3$ meV. This leads to a frequency of $\sim$1000 GHz which validates the adiabatic approximation temporally. Regarding the amplitude condition, we are considering the regimes of the first few plateaus in the acoustoelectric current where the SAW amplitude is small so that the adiabatic condition is also valid.

We note that the combined effect of the confining potential perpendicular to the 2D plane (the α term) and the split gates gives rise to lateral confinement forming the quasi-1D channel. When a SAW is launched in the channel, an electron can be captured in a minimum of the SAW (see Fig. 2) effectively giving rise to a moving quantum dot.

B. Eigenvalues and eigenfunctions

The single-particle Hamiltonian is time dependent and we assume the adiabatic approximation is valid for obtaining the eigenvalues and eigenfunctions, as we did in our previous work.[27] Since we are dealing with SO interaction we need to express the states as spinors. Let $|u_\nu(t)\rangle$ be an instantaneous eigenspinor of $H(t)$ with

$$|u_\nu(t)\rangle = \begin{pmatrix} u_\nu^{(+)}(t) \\ u_\nu^{(-)}(t) \end{pmatrix}, \quad H(t)|u_\nu(t)\rangle = E_\nu(t)|u_\nu(t)\rangle, \tag{8}$$

so that a general spinor can be expanded in terms of the instantaneous eigenspinors as basis, i.e.,

$$|\Psi(t)\rangle = \sum c_\nu(t)|u_\nu(t)\rangle, \tag{9}$$

with coefficients $c_\nu(t)$.

Our objective is to calculate the instantaneous eigenvalues and eigenspinors. Following the procedure presented in Ref. 27, the coefficients $c_\nu(t)$ are determined by

$$\frac{\partial c_\nu(t)}{\partial t} = \sum_{\mu \neq \nu} \frac{c_\mu(t)}{E_\nu(t) - E_\mu(t)} \langle u_\nu(t)| \frac{\partial H(t)}{\partial t} |u_\mu(t)\rangle. \tag{10}$$

Also, the components of the instantaneous eigenspinors satisfy the following set of coupled equations:

$$\left(H_0(t) + i\frac{\beta y}{\lambda_0}\frac{\partial}{\partial x} + i\gamma(x,t)\frac{\partial}{\partial y}\right)u_\nu^{(+)} + i\alpha\left(-i\frac{\partial}{\partial x} - \frac{\partial}{\partial y}\right)u_\nu^{(-)} = E_\nu u_\nu^{(+)}, \tag{11}$$

$$\left(H_0(t) - i\frac{\beta y}{\lambda_0}\frac{\partial}{\partial x} - i\gamma(x,t)\frac{\partial}{\partial y}\right)u_\nu^{(-)} + i\alpha\left(i\frac{\partial}{\partial x} - \frac{\partial}{\partial y}\right)u_\nu^{(+)} = E_\nu u_\nu^{(-)}, \tag{12}$$

where we introduced

$$H_0(t) = \frac{-\hbar^2}{2m^*}\left(\frac{\partial^2}{\partial x^2} + \frac{\partial^2}{\partial y^2}\right) + \frac{\hbar\Omega}{2}\left(\frac{y}{\lambda_0}\right)^2 + H_B(x) + H_{SAW}(x,t). \tag{13}$$

The reason we cannot use separation of variables to reduce the problem as in the paper by Moroz and Barnes[35] is as follows. In Ref. 35, the SAW $[H_{SAW}(x,t)]$ and split-gate potential $[H_B(x)]$ are absent and consequently there is translational invariance along the channel for which there is a plane-wave solution. This allowed one to reduce the equations to two coupled ordinary linear differential equations for the spinor components. However, in our model calculation, due to the presence of the SAW and split gates, there is no such translational invariance and we have coupled partial differential equations which require a different approach. This is described in Sec. III below. Therefore, we cannot separate the x component with the substitution

$$|u_\nu(t)\rangle = e^{ik_x x}|\phi_\nu(t)\rangle \tag{14}$$

to obtain coupled ordinary differential equations as in the paper by Moroz and Barnes.[35]

In addition, due to the SO terms the x and y components of the wave function do not separate. Consequently, we cannot use separation of variables to reduce the problem to a one-dimensional Schrödinger equation. As a result, we have to solve a set of coupled partial differential equations numerically. We note the Rashba α term is responsible for mixing the $(\pm)$ spin states. In the next section, we introduce a simplification regarding the coupling parameters in order to solve the coupled equations without the use of perturbation theory.

III. NONPERTURBATION APPROACH

We first consider the role played by the β and γ-terms of the SO interactions by neglecting the Rashba α coupling. We

do so merely to examine the role these two terms play in modifying the energy eigenvalues although the α term is much stronger than either one of these two terms. In addition, we simplify the calculation by replacing $\beta(y/\lambda_0)\to\bar{\beta}$ and $\gamma(x,t)\to\bar{\gamma}$ which are constants. This is reasonable because even though the lateral parabolic potential is symmetric, it still gives rise to an effect on the energy eigenvalues as shown by Moroz and Barnes.[35] For example, the y coordinate in Eq. (6) is replaced by $\lambda_\beta=\hbar^2/2m^*\beta$ which is the characteristic spatial scale associated with the β coupling. The reason we adopt this approximation is that it simplifies the numerical calculations. In addition, it still allows us to include the SO effects as desired.

The equations we wish to solve are then given by

$$\left[\frac{-\hbar^2}{2m^*}\left(\frac{\partial^2}{\partial x^2}+\frac{\partial^2}{\partial y^2}\right)\pm i\bar{\beta}\frac{\partial}{\partial x}\pm i\bar{\gamma}\frac{\partial}{\partial y}+V(x,t)+\frac{\hbar\Omega}{2}\frac{y^2}{\lambda_0^2}\right]u_\nu^{(\pm)}=E_\nu u_\nu^{(\pm)}. \tag{15}$$

We rewrite the equations in (15) by changing to dimensionless variables defined by $x=l_0\xi$ and $y=\lambda_0\eta$ to obtain

$$\left[V_0\left(-\frac{\partial^2}{\partial\xi^2}\pm i\tilde{\beta}\frac{\partial}{\partial\xi}+\bar{V}(\xi,t)\right)+\frac{\hbar\Omega}{2}\left(-\frac{\partial^2}{\partial\eta^2}\pm i\tilde{\gamma}\frac{\partial}{\partial\eta}+\eta^2\right)\right]u_\nu^{(\pm)}=E_\nu u_\nu^{(\pm)}. \tag{16}$$

Here, $\tilde{\beta}$ and $\tilde{\gamma}$ are dimensionless parameters and $\bar{V}$ is a dimensionless potential. They are given by

$$V_0=\frac{\hbar^2}{2m^*l_0^2},\quad \tilde{\beta}=\frac{\bar{\beta}}{l_0V_0},\quad \tilde{\gamma}=\frac{2\bar{\gamma}}{\lambda_0\hbar\Omega} \tag{17}$$

$$\bar{V}(\xi,t)=\frac{1}{\cosh^2(\xi l_0/l)}+\bar{\Gamma}\cos(kl_0\xi-\omega t). \tag{18}$$

Here, $\bar{\Gamma}=V_{SAW}/V_0$ is the ratio of the piezoelectric potential amplitude to the height of the electrostatic barrier induced by the split gates. These are related to the SAW power and the gate voltage, respectively. When $\bar{\Gamma}$ increases, the current undergoes a rapid increase from zero to its quantized value $I=ef$, where f is the SAW frequency. We can eliminate the first-order derivatives in Eq. (16) by applying the following transformation

$$u^{(\pm)}(\xi,\eta,t)=\tilde{u}^{(\pm)}(\xi,\eta,t)\exp[\pm i/2(\tilde{\beta}\xi+\tilde{\gamma}\eta)]. \tag{19}$$

This leads to a Schrödinger-like equation with shifted energies as follows:

$$\left[V_0\left(-\frac{\partial^2}{\partial\xi^2}+\bar{V}(\xi,t)-\tilde{\beta}^2/4\right)+\frac{\hbar\Omega}{2}\left(-\frac{\partial^2}{\partial\eta^2}\eta^2+\eta^2-\tilde{\gamma}^2/4\right)\right]\tilde{u}_\nu^{(\pm)}=E_\nu\tilde{u}_\nu^{(\pm)}. \tag{20}$$

The differential equations in (20) are separable and are exactly the same as those obtained in the absence of the SO interaction, except for a shift in the energy eigenvalues. These energy eigenvalues are shifted downward by an amount $(V_0\tilde{\beta}^2+\hbar\Omega\tilde{\gamma}^2/2)/4$ and the wave functions in (19) acquire an additional phase factor. We note that the components of the spinor have the same energy eigenvalues, i.e., the β coupling is not capable of lifting the energy degeneracy of the spinor components. This latter result is consistent with that obtained by Moroz and Barnes[35] for a quantum wire with SO coupling.

A. The effect of finite-α coupling

In this section, we shall explore the effect that finite-α coupling has on the energy eigenvalues for confined electrons in the quantum dot. This may be achieved in a nonperturbative approach for the total Hamiltonian $H_{tot}=H(t)+H_{SO}^{\alpha}$, where

$$H_{SO}^{\alpha}=i\alpha\begin{pmatrix}0 & -i\frac{\partial}{\partial x}-\frac{\partial}{\partial y}\\ i\frac{\partial}{\partial x}-\frac{\partial}{\partial y} & 0\end{pmatrix},$$

since we have solutions for the Hamiltonian $H_0(t)$ when this term is neglected. We expand the eigenspinors in terms of the solutions we obtained in the preceding subsection, i.e.,

$$H'(t)'|u_\nu^{\pm}(x,y,t)\rangle=E_\nu^0(t)|u_\nu^{\pm}(x,y,t)\rangle,\qquad |u_\nu^{\pm}(x,y,t)\rangle=|\phi_i^{\pm}(x,t)\chi_m^{\pm}(y)\rangle,\qquad E_\nu^0=\varepsilon_{xi}^0(t)+\varepsilon_{ym}^0. \tag{21}$$

Here, $\chi_m^{\pm}(y)$ are harmonic oscillator eigenfunctions and the $\phi_i^{\pm}(x,t)$ are evaluated numerically. We start by writing the eigenspinor components as follows:

$$\Phi^{(\pm)}=\sum_{\nu=0}^{\infty}c_\nu^{(\pm)}u_\nu^{(+)},$$

$$\Phi^{(\pm)}=\sum_{\nu=0}^{\infty}d_\nu^{(\pm)}u_\nu^{(-)}. \tag{22}$$

Substituting these equations into the original equation we get

$$\sum_{\nu=0}^{\infty}c_\nu^{(+)}u_\nu^{(+)}E_\nu^0+\frac{\alpha}{\hbar}\sum_{\nu=0}^{\infty}c_\nu^{(-)}(ip_x+p_y)u_\nu^{(+)}=E\sum_{\nu=0}^{\infty}c_\nu^{(+)}u_\nu^{(+)}, \tag{23}$$

$$\sum_{\nu=0}^{\infty}d_\nu^{(-)}u_\nu^{(-)}E_\nu^0+\frac{\alpha}{\hbar}\sum_{\nu=0}^{\infty}d_\nu^{(+)}(-ip_x+p_y)u_\nu^{(-)}=E\sum_{\nu=0}^{\infty}d_\nu^{(-)}u_\nu^{(-)}. \tag{24}$$

Taking the inner products $\langle u^{(+)}\mu|$ and $\langle u_\mu^{(-)}|$, respectively, we obtain

$$c_\mu^{(+)}(E_\mu^0-E)+\frac{\alpha}{\hbar}\sum_{\nu=0}^{\infty}c_\nu^{(-)}\langle u_\mu^{(+)}|(ip_x+p_y)|u_\nu^{(+)}\rangle=0, \tag{25}$$

$$d_\mu^{(-)}(E_\mu^0 - E) + \frac{\alpha}{\hbar}\sum_{\nu=0}^{\infty} d_\nu^{(+)}\langle u_\mu^{(-)}|(-ip_x + p_y)|u_\nu^{(-)}\rangle = 0. \quad (26)$$

We evaluate the matrix elements using the following relationships:

$$p_x = \frac{m^*}{i\hbar}[x,H'] \pm \frac{m^*\bar{\beta}}{\hbar}, \quad p_y = \frac{m^*}{i\hbar}[y,H'] \pm \frac{m^*\bar{\gamma}}{\hbar}. \quad (27)$$

Exploiting these results, we obtain the following:

$$c_\mu^{(+)}(E_\mu^0 - E) + \sum_{\nu=0}^{\infty} c_\nu^{(-)}(\Delta_{\mu,\nu}^{x(+)} + \Delta_{\mu,\nu}^{y(+)} + \epsilon_{\mu,\nu}^{(+)}) = 0, \quad (28)$$

$$d_\mu^{(-)}(E_\mu^0 - E) + \sum_{\nu=0}^{\infty} d_\nu^{(+)}(\Delta_{\mu,\nu}^{x(-)} + \Delta_{\mu,\nu}^{y(-)} + \epsilon_{\mu,\nu}^{(-)}) = 0. \quad (29)$$

Here we have defined

$$\epsilon_{\mu,\nu}^{(\pm)} = \frac{m^*\alpha}{\hbar^2}(\bar{\gamma} \pm i\bar{\beta})\delta_{\mu,\mu} = \epsilon^{(\pm)}, \quad (30)$$

$$\Delta_{\mu\nu}^{(x\pm)} = \pm\frac{m^*\alpha}{\hbar^2}(E_\nu^0 - E_\mu^0)x_{\mu,\nu}^{(\pm)}, \quad (31)$$

$$\Delta_{\mu\nu}^{y(\pm)} = \frac{m^*\alpha}{i\hbar^2}(E_\nu^0 - E_\mu^0)y_{\mu,\nu}^{(\pm)}. \quad (32)$$

Here, $x_{\mu,\nu}^{\pm} = \langle u_\mu^{(\pm)}|x|u_\nu^{(\pm)}\rangle$ and $y_{\mu,\nu}^{\pm} = \langle u_\mu^{(\pm)}|y|u_\nu^{(\pm)}\rangle$ are the unperturbed matrix elements which are evaluated numerically. We solve these equations for the lowest states in the SAW minima $[\phi_{i=0}(x,t)]$. Numerical calculation of the x matrix elements including the energy difference prefactor in Eq. (31) shows that these terms are small in comparison to the other matrix elements and can be neglected. The y matrix elements can be evaluated analytically as follows:

$$\langle u_\mu^{(\pm)}|y|u_\nu^{(\pm)}\rangle = \langle \tilde{u}_\mu|\eta|\tilde{u}_\nu\rangle \quad (33)$$

$$= \langle \phi(\xi,t)_j|\phi_i(\xi,t)\rangle\langle\chi(\eta)_n|\eta|\chi_m(\eta)\rangle \quad (34)$$

$$= \frac{\lambda_0}{\sqrt{2}}(\sqrt{m}\delta_{n,m-1} + \sqrt{m+1}\delta_{n,m+1}). \quad (35)$$

The equations are then reduced to a set of infinite algebraic equations,

$$c_{n,0}^{(+)}(E_{n,0}^0 - E) + c_{n+1,0}^{(-)}\Delta_{n,n+1}^{y(+)} + c_{n-1,0}^{(-)}\Delta_{n,n-1}^{y(+)} + c_{n,0}^{(-)}\epsilon^{(+)} = 0, \quad (36)$$

$$d_{n,0}^{(-)}(E_{n,0}^0 - E) + d_{n+1,0}^{(+)}\Delta_{n,n+1}^{y(-)} + d_{n-1,0}^{(+)}\Delta_{n,n-1}^{y(-)} + d_{n,0}^{(+)}\epsilon^{(-)} = 0. \quad (37)$$

We can solve these equations using the method employed in Ref. 35:

$$\mathbf{c}^+ = \hat{U}^+\mathbf{c}^-, \quad (38)$$

$$\mathbf{d}^- = \hat{U}^-\mathbf{d}^+. \quad (39)$$

Here, $\mathbf{c}^\pm$ and $\mathbf{d}^\pm$ are vector coefficients and the elements of the matrices $\hat{U}^\pm$ are given by

$$U_{n,n}^{(\pm)} = \frac{\epsilon^{(\pm)}}{(E - E_{n,0}^0)}, \quad (40)$$

$$U_{n,n+1}^{(\pm)} = \kappa\sqrt{\frac{n+1}{2}}\frac{1}{E - E_{n,0}^0}, \quad (41)$$

$$U_{n+1,n}^{(\pm)} = -\kappa\sqrt{\frac{n+1}{2}}\frac{1}{E - E_{n+1,0}^0}. \quad (42)$$

Here $\epsilon^{(\pm)} = \alpha(\bar{\gamma} \pm i\bar{\beta})/\lambda_0^2\hbar\Omega$ and $\kappa = \alpha/i\lambda_0$. By taking inner products of Eqs. (22) we obtain a relationship between the $\mathbf{c}$'s and $\mathbf{d}$'s,

$$\mathbf{c}^\pm = \hat{W}^+\mathbf{d}^\pm, \quad (43)$$

$$\mathbf{d}^\pm = \hat{W}^-\mathbf{c}^\pm. \quad (44)$$

Combining the above we obtain the following:

$$\mathbf{c}^+ = \hat{U}^+\mathbf{c}^- \quad (45)$$

$$= \hat{U}^+\hat{W}^+\mathbf{d}^- \quad (46)$$

$$= \hat{U}^+\hat{W}^+U^-\mathbf{d}^+ \quad (47)$$

$$= \hat{U}^+\hat{W}^+\hat{U}^-\hat{W}^-\mathbf{c}^+. \quad (48)$$

The eigenvalues of this equation yield the energies,

$$\det(1 - \hat{U}^+\hat{W}^+\hat{U}^-\hat{W}^-) = 0. \quad (49)$$

The resulting matrix is truncated to obtain an $n \times n$ matrix followed by a numerical root finder to obtain the energy eigenvalues. However, we can see the effect by considering the leading term (letting $\Delta^\pm = 0$) which yields the following:

$$\begin{vmatrix} 1 - \epsilon^{(+)}\epsilon^{(-)}/(E - E_{0,0}^0)^2 & 0 & \cdots \\ 0 & 1 - \epsilon^{(-)}\epsilon^{(+)}/(E - E_{1,0}^0)^2 & \\ \vdots & 0 & \ddots \end{vmatrix} = 0 \quad (50)$$

giving

$$1 - \left(\frac{m^*\alpha}{\hbar^2}\right)^2(\bar{\gamma} + i\bar{\beta})(\bar{\gamma} - i\bar{\beta})/(E - E_n^0)^2 = 0, \quad (51)$$

$$\Delta E_{n,0}^{\pm} = \pm\frac{m^*\alpha}{\hbar^2}\sqrt{\bar{\beta}^2 + \bar{\gamma}^2}. \quad (52)$$

Unlike the model for a quantum wire used by Moroz and Barnes,[35] the eigenfunctions along the channel have discrete spectra due to the confinement by the SAW potential and split gate. We note that due to the α coupling, the spinor states are decoupled. The result of neglecting the off-diagonal terms is identical to the result of first-order perturbation corrections to the energy eigenvalues. First-order perturbation yields

$$\begin{vmatrix} \Delta E_\nu & \alpha\left\langle u_\nu^+ \left| \frac{\partial u_\nu^-}{\partial x} \right\rangle - i\alpha \left\langle u_\nu^+ \left| \frac{\partial u_\nu^-}{\partial y} \right\rangle \right. \right. \\ -\alpha\left\langle u_\nu^- \left| \frac{\partial u_\nu^+}{\partial x} \right\rangle - i\alpha \left\langle u_\nu^- \left| \frac{\partial u_\nu^+}{\partial y} \right\rangle \right. \right. & \Delta E_\nu \end{vmatrix} = 0, \tag{53}$$

which yields

$$\Delta E_\nu^\pm = \pm \alpha \left[\left(\left\langle u_\nu^+ \left| \frac{\partial u_\nu^-}{\partial x} \right\rangle - i \left\langle u_\nu^+ \left| \frac{\partial u_\nu^-}{\partial y} \right\rangle \right. \right. \right) \left(- \left\langle u_\nu^- \left| \frac{\partial u_\nu^+}{\partial x} \right\rangle - i \left\langle u_\nu^- \left| \frac{\partial u_\nu^+}{\partial y} \right\rangle \right. \right. \right) \right]^{1/2}. \tag{54}$$

Equation (54) requires that we evaluate the matrix elements involving the solutions $\phi(x,t)$ and $\chi(y)$ obtained in Sec. III A and can readily be employed to evaluate the above matrix elements. The result is

$$\Delta E_\nu^\pm = \pm \frac{\alpha m^*}{\hbar^2} (\bar{\beta}^2 + \bar{\gamma}^2)^{1/2}, \tag{55}$$

which is identical to the leading term Eq. (52) obtained from Eq. (49) by setting the off-diagonal terms zero. In Figs. 3 and 4, we present the eigenvalues obtained from Eq. (49) at $t=0$. We note from Eq. (55) that for $\bar{\gamma}=0$ we have a linear increase of the split energy as a function of $\bar{\beta}$. We obtain a similar linear law for $\bar{\gamma}$ when $\bar{\beta}=0$.

IV. DISCUSSION OF NUMERICAL RESULTS

The results presented in Figs. 3 and 4 clearly show the effect of SO interaction on the energy eigenvalues of a captured electron in a SAW quantum dot. In Fig. 3, we see twofold spin degeneracy of all quantum levels at $\tilde{\beta}=0$. As the value of $\tilde{\beta}$ is increased from $\tilde{\beta}=0$, the SO interaction lifts the degeneracy and produces an energy splitting $\Delta E_\nu^+ - \Delta E_\nu^-$ which increases linearly with $\tilde{\beta}$, consistent with Eq. (55). Figure 4 is a plot of the energy eigenvalues as a function of α for the states within the quantum dot. We emphasize that the results in Figs. 3 and 4 are only valid for small α but nevertheless present results showing that the energies *cross* for large $\tilde{\beta}$ and α. In this regime, the perturbation approach is not valid and an exact calculation which we described above

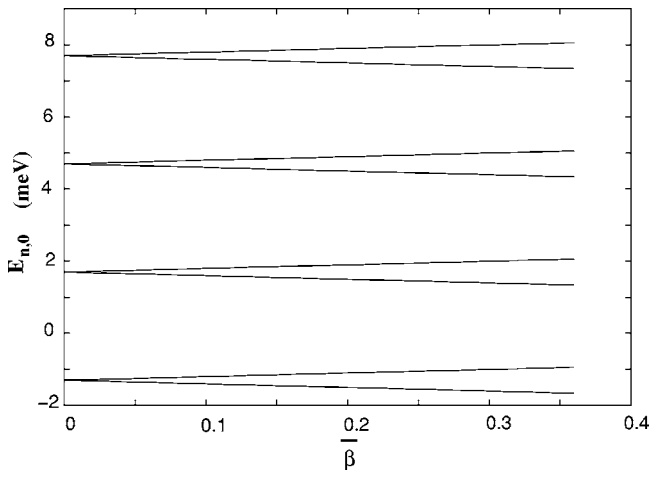

FIG. 3. The lowest energy eigenvalues $E_{n,0}$ (in meV), obtained from Eq. (49), at $t=0$ for finite $\alpha=10$ meV nm as a function of the dimensionless parameter $\tilde{\beta}$. Here, the energy eigenvalues are labeled by n, the quantum number for the harmonic oscillator levels, and 0 which denotes the lowest SAW level. We chose $\tilde{\gamma}=0$.

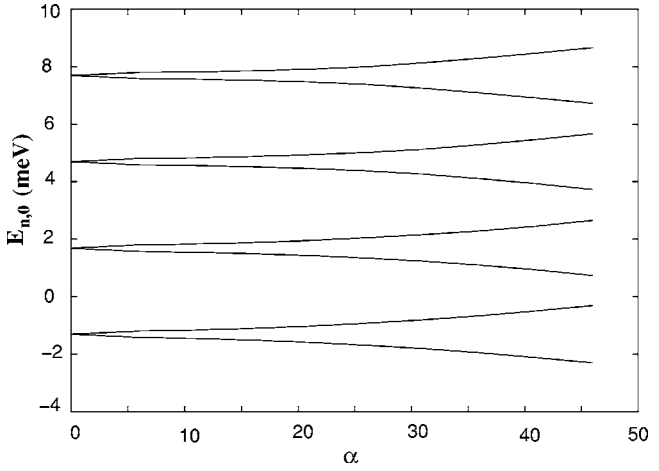

FIG. 4. The lowest-energy eigenvalues $E_{n,0}$ (in meV) obtained from Eq. (49) at $t=0$ for finite $\tilde{\beta}=0.1$ as a function of the parameter α. Here, the energy eigenvalues are labeled by n, the quantum number for the harmonic oscillator levels, and 0 which denotes the lowest SAW level. We chose $\tilde{\gamma}=0$.

must be used. As a matter of fact, the eigenvalues must bend and lead to *anticrossing* of branches corresponding to neighboring energy levels. Since we are not interested in this detailed behavior, we do not solve the eigenvalue problem exactly because our main goal is to demonstrate the lifting of the degeneracy and a decrease of the energy eigenvalues by the Rashba SO interaction. We have presented results at $t=0$ only but the acoustoelectric current is determined over an entire SAW cycle. We have verified that our conclusions do not depend on time.

V. CONCLUDING REMARKS

The recent development in experimental realization of Q1D systems driven by SAWs exhibit many interesting features such as current quantization and have potential applications as a current standard and quantum information and security schemes. In this paper, we investigated the effect of SO interaction on the electron energy levels which play a crucial role in determining the acoustoelectric current. The SO interaction may arise from the electrostatic confining potential of the SAW as well as the split gates and the heterostructure. The simplified calculation we used was able to show that the SO interaction splits the energy levels. By treating the α parameter as a continuous variable, we carried out calculations only for small α. To obtain the full effect of the α term, one has to employ a nonperturbative approach. However, we are principally interested in demonstrating its effect in lowest order.

Also, as the β and γ parameters are increased, the energy eigenvalues are slightly increased when α is set equal to zero. However, finite α lifts the degeneracy of the levels and one of the split energy levels is decreased as shown in Figs. 3 and 4. This implies that the SO interaction can produce spin currents and that the electron tunneling probability for the lower of the two split levels is decreased (see Fig. 1). A decrease in probability of being transported through the channel may lead to a finite slope in the acoustoelectric current plateau. Furthermore, additional theoretical and experimental studies to examine related problems that would affect the performance of these devices, such as spin coherence, should be carried out. Finally, the calculations we reported on the SO Hamiltonian were not calculated self-consistently to determine the confining potential and the eigenstates. Such a self-consistent calculation should not yield results that are qualitatively different from those presented above.

ACKNOWLEDGMENTS

The authors acknowledge partial support from the National Science Foundation under Grant No. CREST 0206162 and PSC-CUNY Grant No. 65485-00-34.

*Electronic address: ggumbs@hunter.cuny.edu
†Electronic address: yabranyo@hunter.cuny.edu

[1] L. P. Kouwenhoven, D. G. Austing, and S. Tarucha, Rep. Prog. Phys. **64**, 701 (2001); L. P. Kouwenhoven and C. M. Marcus, Phys. World **11**(6), 35 (1998).
[2] M. A. Kastner, Ann. Phys. (N.Y.) **9**, 885 (2000).
[3] U. Mackens, D. Heitmann, L. Prager, and J. P. Kotthaus, and W. Beinvogl, Phys. Rev. Lett. **53**, 1485 (1984).
[4] D. Loss and D. P. DiVincenzo, Phys. Rev. A **57**, 120 (1998); Guido Burkard, Daniel Loss, and David P. DiVincenzo, Phys. Rev. B **59**, 2070 (1999).
[5] J. M. Elzerman, R. Hanson, L. H. Willems van Beveren, B. Witkamp, L. M. K. Vandersypen, and L. P. Kouwenhoven, Nature (London) **430**, 431 (2004).
[6] C. H. W. Barnes, J. M. Shilton, and A. M. Robinson, Phys. Rev. B **62**, 8410 (2000); C. H. W. Barnes, Philos. Trans. R. Soc. London, Ser. A **361**, 1487 (2003).
[7] V. I. Talyanskii, J. M. Shilton, M. Pepper, C. G. Smith, C. J. B. Ford, E. H. Linfield, D. A. Ritchie, and G. A. C. Jones, Phys. Rev. B **56**, 15180 (1997).
[8] J. M. Shilton, V. I. Talyanskii, M. Pepper, D. A. Ritchie, J. E. F. Frost, C. J. B. Ford, C. G. Smith, and G. A. C. Jones, J. Phys.: Condens. Matter **8**, L531 (1999).
[9] V. I. Talyanskii, J. M. Shilton, M. Pepper, C. G. Smith, C. J. B. Ford, E. H. Linfield, D. A. Ritchie, and G. A. C. Jones, Phys. Rev. B **56**, 15180 (1997).
[10] V. I. Talyanskii, J. M. Shilton, J. Cunningham, M. Pepper, C. J. B. Ford, C. G. Smith, E. H. Linfield, D. A. Ritchie, and G. A. C. Jones, Physica B **251**, 140 (1998).
[11] J. Cunningham, V. I. Talyanskii, J. M. Shilton, M. Pepper, M. Y. Simmons, and D. A. Ritchie, Phys. Rev. B **60**, 4850 (1999).
[12] J. Cunningham, V. I. Talyanskii, J. M. Shilton, M. Pepper, A. Kristensen, and P. E. Lindelof, Physica B **280**, 493 (2000).
[13] N. E. Fletcher, J. Ebbecke, T. J. B. M. Janssen, F. J. Ahlers, M. Pepper, H. E. Beere, and D. A. Ritchie, Phys. Rev. B **68**, 245310 (2003).
[14] Yukinori Ono, Akira Fujiwara, Katsuhiko Nishiguchi, Hiroshi Inokawa, and Yasuo Takahashi, J. Appl. Phys. **97**, 031101 (2005).
[15] J. Cunningham, M. Pepper, V. I. Talyanskii, and D. A. Ritchie, Appl. Phys. Lett. **86**, 152105 (2005).
[16] M. M. de Lima, Jr., R. Hey, J. A. H. Stotz, and P. V. Santos, Appl. Phys. Lett. **84**, 2569 (2004).
[17] C. L. Foden, V. I. Talyanskii, G. J. Milburn, M. L. Leadbeater, and M. Pepper, Phys. Rev. A **62**, 011803(R) (2000).
[18] T. Hosey, V. Talyanskii, S. Vijendran, G. A. C. Jones, M. B. Ward, D. C. Unitt, C. E. Norman, and A. J. Shields, Appl. Phys. Lett. **85**, 491 (2004).
[19] G. R. Aizin, G. Gumbs, and M. Pepper, Phys. Rev. B **58**, 10589 (1998); G. Gumbs, G. R. Aizin, and M. Pepper, *ibid.* **60**, R13954 (1999).
[20] A. M. Robinson, V. I. Talyanskii, M. Pepper, J. E. Cunningham, E. H. Linfield, and D. A. Ritchie, Phys. Rev. B **65**, 045313 (2002).
[21] Y. M. Galperin, O. Entin-Wohlman, and Y. Levinson, Phys. Rev. B **63**, 153309 (2001).
[22] J. Cunningham, V. I. Talyanskii, J. M. Shilton, M. Pepper, A. Kristensen, and P. E. Lindelof, Phys. Rev. B **62**, 1564 (2000).
[23] N. A. Zimbovskaya and G. Gumbs, J. Phys.: Condens. Matter **13**,

L409 (2001).
[24] Yu. A. Bychkov and E. I. Rashba, J. Phys. C **17**, 6039 (1984).
[25] A. Ghosh, M. H. Wright, C. Siegert, M. Pepper, I. Farrer, C. J. B. Ford, and D. A. Ritchie, Phys. Rev. Lett. **95**, 066603 (2005).
[26] A. Ghosh, C. J. B. Ford, M. Pepper, H. E. Beere, and D. A. Ritchie, Phys. Rev. Lett. **92**, 116601 (2004).
[27] G. Gumbs and Yonatan Abranyos, Phys. Rev. A **70**, 050302(R) (2004).
[28] G. Dresselhaus, Phys. Rev. **100**, 580 (1955).
[29] J. Luo, H. Munekata, F. F. Fang, and P. J. Stiles, Phys. Rev. B **41**, 7685 (1990).
[30] B. Jusserand, D. Richards, H. Peric, and B. Etienne, Phys. Rev. Lett. **69**, 848 (1992).
[31] A. G. Mal'shukov, K. A. Chao, and M. Willander, Phys. Rev. Lett. **76**, 3794 (1996).
[32] M. Governale, F. Taddei, and Rosario Fazio, Phys. Rev. B **68**, 155324 (2003).
[33] C. S. Tang, A. G. Mal'shukov, and K. A. Chao, Phys. Rev. B **71**, 195314 (2005).
[34] C. S. Tang and C. S. Chu, Solid State Commun. **120**, 353 (2001).
[35] A. V. Moroz and C. H. W. Barnes, Phys. Rev. B **60**, 14272 (1999); **61**, R2464 (2000); A. V. Moroz, K. V. Samokhin, and C. H. W. Barnes, Phys. Rev. Lett. **84**, 4164 (2000).